

Article

# $\alpha$ - Synuclein amyloid fibrils investigation with the use of fluorescent probe thioflavin T

Anna I. Sulatskaya<sup>1</sup>, Natalia P. Rodina<sup>1</sup>, Maksim I. Sulatsky<sup>1</sup>, Olga I. Povarova<sup>1</sup>,  
Iuliia A. Antifeeva<sup>1</sup>, Irina M. Kuznetsova<sup>1</sup>, Konstantin K. Turoverov<sup>1,2,\*</sup>

<sup>1</sup> Laboratory of Structural dynamics, stability and folding of proteins, Institute of Cytology of the Russian Academy of Science, St. Petersburg, Tikhoretsky ave. 4, 194064, Russia

<sup>2</sup> Institute of Physics, Nanotechnology and Telecommunications, Peter the Great St.-Petersburg Polytechnic University, St. Petersburg, Polytechnicheskaya 29, 195251, Russia

\* Correspondence: kkt@incras.ru; Tel.: +7-812-297-19-57

**Abstract:** In this work  $\alpha$ -synuclein amyloid fibrils, formation of which is a biomarker of the Parkinson's disease, were investigated with the use of fluorescent probe thioflavin T (ThT). Experimental conditions of the protein fibrillogenesis were chosen so that a sufficient number of continuous measurements can be performed to characterize and analyze all stages of this process. The reproducibility of fibrillogenesis and the structure of the obtained aggregates (that is a critical point for their further investigation) were proved using a wide range of physical-chemical methods. For determination of ThT -  $\alpha$ -synuclein amyloid fibrils binding parameters sample and reference solutions were prepared with the use of equilibrium microdialysis. By absorption spectroscopy of these solutions ThT – fibrils binding mode with the binding constant about  $10^4$  M<sup>-1</sup> and stoichiometry of ThT per protein molecule about 1:8 was observed. Fluorescence spectroscopy of the same solutions with the subsequent correction of the recorded fluorescence intensity on the primary inner filter effect allowed to determine another mode of ThT binding to fibrils with the binding constant about  $10^6$  M<sup>-1</sup> and stoichiometry about 1:2500. Analysis of photophysical characteristics of the dye molecules bound to the sites of different binding modes allowed to assume the possible localization of these sites. Obtained differences in the ThT binding parameters to amyloid fibrils formed from  $\alpha$ -synuclein and other amyloidogenic proteins, as well as in the photophysical characteristics of the bound dye, confirmed the hypothesis of amyloid fibrils polymorphism.

**Keywords:**  $\alpha$ -synuclein, amyloid fibrils, fibrillogenesis, thioflavin T, equilibrium microdialysis, binding parameters, structural polymorphism

## 1. Introduction

$\alpha$ -Synuclein (Figure 1a) is a small soluble protein consisting of 140 amino acid residues [1, 2] that is mainly synthesized in the central nervous system [3, 4], but as well can be found in the periphery, e.g. in erythroid cells [5, 6], platelets [7, 8] and lymphocytes [9]. The physiological role of  $\alpha$ -synuclein is highly diverse: it is assigned to the microtubule-associated activity [10], antioxidant activity in membranes [11], a role in neuronal plasticity [12], functioning as a molecular chaperone in the formation of SNARE-complexes [13], as well as involved in the functioning of the Golgi apparatus and transport vesicles [14], etc. A wide range of  $\alpha$ -synuclein functions is in a good agreement with the fact that it is a hub protein. Hub proteins are characterized by high conformational plasticity that gives them the opportunity to change their spatial configuration depending on the environment and interact with a large number of partners. For  $\alpha$ -synuclein more than 30 partners were identified [15].

As many hub proteins [16],  $\alpha$ -synuclein is an intrinsically disordered protein that has no pronounced secondary structure in aqueous solutions [17, 18]. While binding to its partners,  $\alpha$ -synuclein can acquire significantly more compact structures [19]. One of the best characterized  $\alpha$ -synuclein folds is the membrane or vesicle bound  $\alpha$ -helical conformation [20-23]. Recently, a tetrameric form of  $\alpha$ -synuclein with stable helical structure, that is suggested to play an important role in the protein homeostasis, was discovered [18, 24].

It is thought, that disturbance of the protein interaction with its natural partners by the influence of various endogenous and exogenous factors including mutations, leads to association of  $\alpha$ -synuclein molecules with formation of ordered aggregates and occurrence of amyloid fibrils [18, 19, 25, 26].  $\alpha$ -Synuclein fibril formation is a nucleation-dependent process in which the rate-limiting step is the spontaneous formation of small metastable oligomeric intermediates, called amyloid cores [27]. As it was shown in the latest researches, the initially formed proteinase K-sensitive amyloid oligomers slowly converse into more stable proteinase K-resistant oligomers [28] proceeding protofibrils formation. These protofibrils can interact with each other with formation of highly polymorphic  $\alpha$ -synuclein amyloid fibrils [29, 30].

Aggregated  $\alpha$ -synuclein is the major component of pathological Lewy bodies in Parkinson's disease and dementia (DLB) as well as amyloid plaques in Alzheimer's disease [15, 27]. However, the processes underlying  $\alpha$ -synuclein aggregation and its pathological appearance are currently not well understood. Elucidation of the molecular mechanisms of  $\alpha$ -synuclein amyloidosis (synucleinopathys), study of the deposits properties, elaboration of methods of *in vivo* diagnosis of these pathological inclusions and development of therapeutic treatment are urgent tasks. Successful solution of these problems depends largely on our knowledge about the physico-chemical properties, structural features and formation mechanism of  $\alpha$ -synuclein amyloid fibrils as well as about the mechanisms of their interaction with potential diagnostic and therapeutic agents.

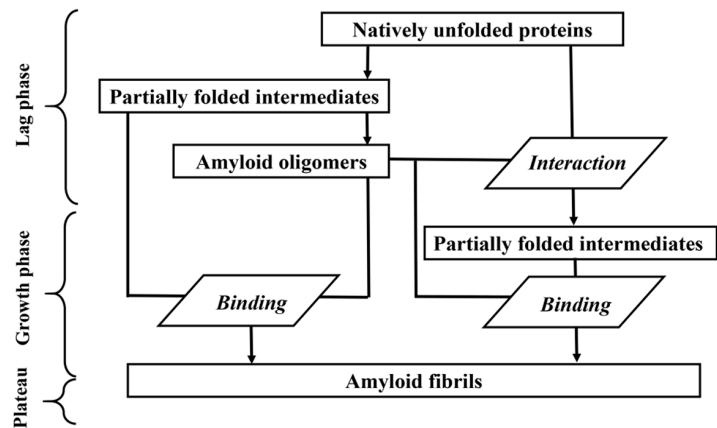
One of the widely used tools for the diagnosis of amyloid fibrils, and, recently, for investigation of their structure is the benzothiazole dye thioflavin T (ThT) [31-35]. This is due to the specificity of the dye interaction with amyloid fibrils and significant difference of its photophysical characteristics in the free and bound to fibrils state. Recent works showed that determination of ThT – amyloid fibrils binding parameters can be used for investigation of their structure [34-36]. However, as we know there are no studies where stoichiometry and affinity of the dye interaction with  $\alpha$ -synuclein amyloid fibrils were evaluated correctly. In most studies of ThT binding parameters to amyloid fibrils formed from  $\alpha$ -synuclein and other proteins the dependence of the dye fluorescence intensity on its total concentration was used instead of the concentration of the free dye, as it should be [37-40]. In addition, in these studies, the influence of the inner filter effect on the detected fluorescence intensity was either not taken into account at all, or was performed incorrectly. To solve these problems, in the present work a specially elaborated approach based on spectral investigation of the solutions prepared by equilibrium microdialysis [41] and specially developed method of inner filter effect correction [42] were used. The applicability of the proposed method for binding stoichiometry and affinity determination was earlier demonstrated in study of the ThT interaction with amyloid fibrils formed from the different amyloidogenic proteins [41, 43] and fluorescent dye 8-Anilino-1-naphthalenesulfonic acid (ANS) with serum albumins [44].

In the present work approaches mentioned above were used for estimation of ThT -  $\alpha$ -synuclein amyloid fibrils binding parameters. For determination of  $\alpha$ -synuclein fibrillogenesis duration in the experimental conditions, as well as to verify the reproducibility of this process and the structure of the obtained aggregates the kinetics of fibrils formation and mature aggregates was preliminarily monitored using the wide range of physical-chemical methods.

## 2. Results and Discussion

### 2.1. Kinetics of $\alpha$ -synuclein fibrillation

Analysis of the results of the investigation of amyloid fibrils formation in different conditions presented in the previous work [45] allows to suggest a scheme of  $\alpha$ -synuclein fibrillation (Scheme



**Scheme I.** Scheme of a-synuclein fibrillogenesis. Created on the basis of the results of the work [45].

I). It should be noted that the conditions of fibrillogenesis can significantly affect both the kinetics of this process and the properties of mature amyloid fibrils. The reproducibility of fibrillogenesis, and hence the structure of mature amyloid fibrils is an important point for their further investigation. The most optimal duration of fibrillogenesis to study various parameters of this process is from several hours to 24 hours, since during this period a sufficient number of continuous measurements can be performed to characterize and analyze all stages of this process. However, it turned out that under physiological conditions,  $\alpha$ -synuclein fibrillogenesis is continued for more than three days [45]. At the same time duration of this process is significantly reduced at high temperatures or acidic pH conditions. Taking into account the mentioned above time limits,  $\alpha$ -synuclein fibrillogenesis was performed at pH 3.7 in 0.2 M acetate buffer with constant stirring at 37 °C.

$\alpha$ -Synuclein fibrillogenesis was visualized by electron microscopy (Fig. 1) and changes in the protein secondary structure were monitored by CD-spectroscopy (Fig. 2A). The far-UV CD spectrum of the monomeric  $\alpha$ -synuclein is typical of a predominantly unfolded protein that is proved by a strong negative band around 200 nm [46]. Nevertheless, a weak negative band, appearing as a shoulder around 220 nm, allows to suggest the presence of secondary structure elements in the monomeric protein. Upon fibrillogenesis,  $\alpha$ -synuclein goes from a conformation that is predominantly random to a conformation with considerable beta-structure, as revealed by the

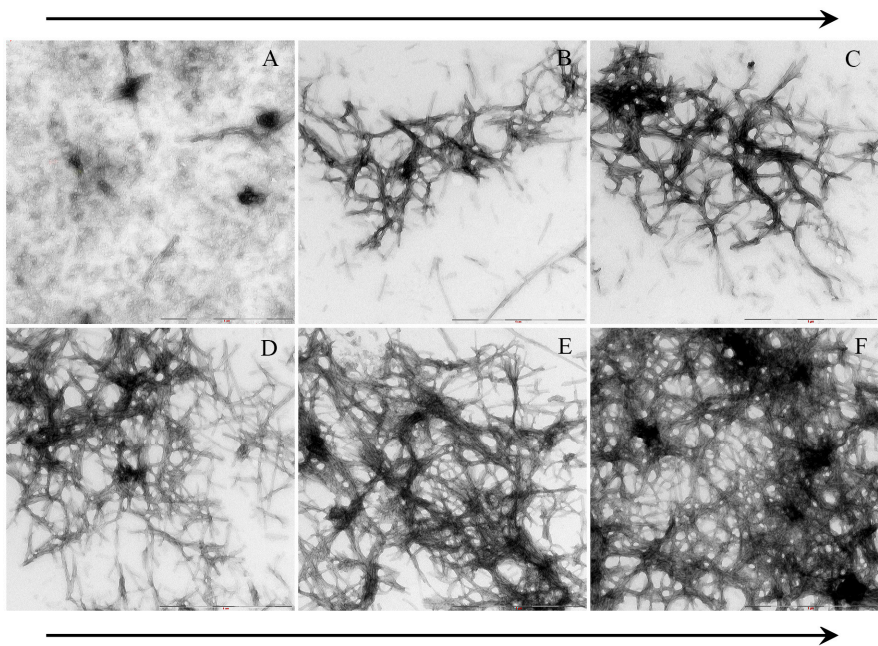


**Figure 1.** Electron micrographs of  $\alpha$ -synuclein during protein fibrillogenesis. Scale bar is 1  $\mu$ m.

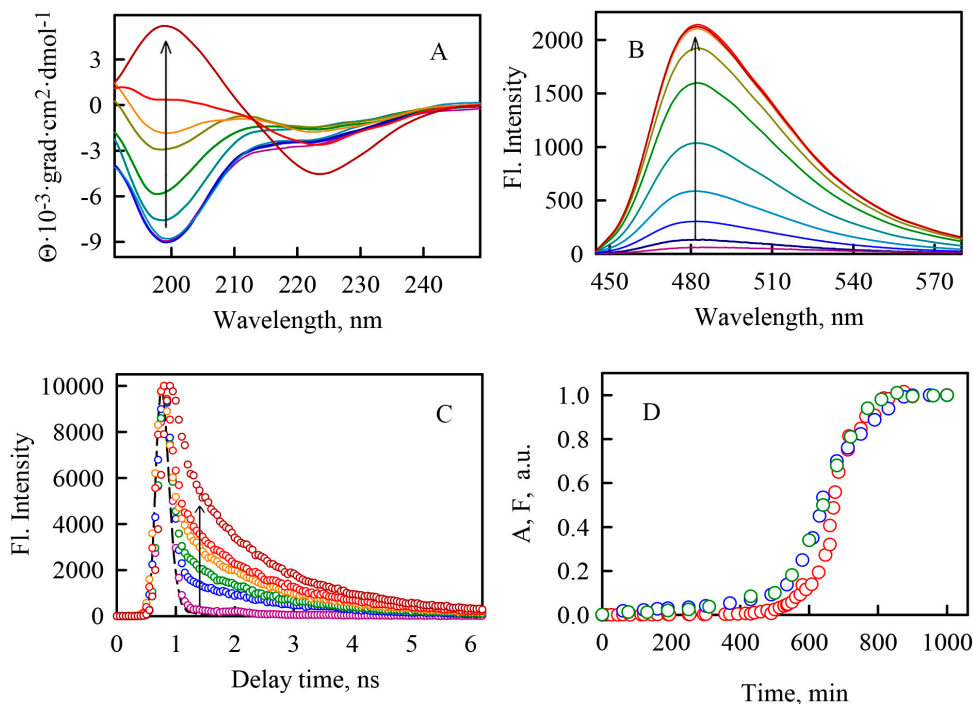


**Figure 2.** Time-dependent change of the different parameters of fluorescent probe thioflavin T (ThT) during  $\alpha$ -synuclein fibrillogenesis. Arrows indicate the direction of change (A) the CD spectra of  $\alpha$ -synuclein at 0, 190, 310, 430, 670, 710, 790, 830, 880 and 1000 min, (B) ThT fluorescence spectra at 510, 560, 610, 650, 670, 710, 790, 880, 950 and 1000 min, (C) ThT fluorescence decay curves at 480, 610, 650, 710, 850 and 1000 min after the start of the fibrillogenesis. The instrument response function is presented by the black dashed line. The panel (D) shows the time dependences of fluorescence (red circles), fluorescence excitation (blue circles) and absorption (green circles) at the maxima of the corresponding spectra.

concomitant intensity decrease of the 200 nm band and increase of the 220 nm band.

Kinetics of amyloid fibrils formation is widely monitored by the fluorescence enhancement of a specific probe thioflavin T (ThT) (Fig. 2B) (see, for example, [47]). In this work, we studied this process in addition by the registration of other ThT photophysical characteristics: fluorescence decay curves (Fig. 2C), absorption and fluorescence excitation (Fig. 2D). Figure 2D shows the same sigmoid character of the time-dependent increase of the different detected parameters. The kinetic curves can be divided into 3 regions: the first (lag phase) is characterized by the ThT parameters invariability, the second is characterized by their increase and the third is characterized by their plateau.

Our results show that in the lag phase which corresponds to formation of the nucleus (Scheme 1) no significant changes in the secondary structure of  $\alpha$ -synuclein occur. The second region of the dependence is characterized by the growth (elongation) of amyloid fibrils. At this stage significant changes in the secondary structure of the protein and in particular an increase in the beta-sheets content was observed. It should be noted that the obtained results do not agree with the some existing ideas that the elongation of amyloid fibrils occurs due to interaction with the seeding of protein ring-like oligomers formed in the lag phase (rather than monomeric proteins) [48]. In this fibrillogenesis scheme, structural transformations should occur, leading to the transition of the most protein amount from the partially folded state to the state of amyloid oligomers, which should be reflected in a significant change in the CD spectra in the lag phase. However, such changes were not observed.

According to obtained results in the lag phase of  $\alpha$ -synuclein fibrillogenesis, only a very small part of the proteins is involved in formation of amyloid oligomers by the partially folded intermediates while the bulk of the proteins remains in the monomeric form. This is due to the fact that spontaneous formation of such oligomers is a long and low-probability process (that is proved



by the relatively prolonged lag phase). Thereby an insignificant change in the secondary structure of the sample in lag phase is caused by a negligible contribution of a small amount of molecules that changed their structure and formed nucleus to the total CD spectrum. At the same time, the formed nucleation core can further act as a "matrix" for structural changes of other  $\alpha$ -synuclein molecules (in particular, as it was previously shown for prions [49]). In the growth phase, addition of partially folded intermediates to amyloid oligomers takes place that leads to a change in monomer proteins secondary structure toward an increase in the content of beta-sheets.

Obtained results show that the kinetics dependence reaches a plateau that is caused by saturation of the ThT binding sites and the formation of mature amyloid fibrils, in about 15 hours. In this connection, for the amyloid fibrils preparation for the following experiments,  $\alpha$ -synuclein was incubated under the chosen conditions for at least 24 hours.

Figure 1 shows that mature  $\alpha$ -synuclein fibrils are unbranched structures, consisting of several protofibrils what is typical for fibrils on the basis of many other amyloidogenic proteins [50-52]. In addition it was observed that increasing time of the fibril incubation does not change their diameter (that is about 10 - 20 nm) while their length increases to 1000 nm. It can be noted that the mature  $\alpha$ -synuclein fibrils tend to interact with each other forming clusters.

## 2.2. ThT- $\alpha$ -synuclein amyloid fibrils binding parameters

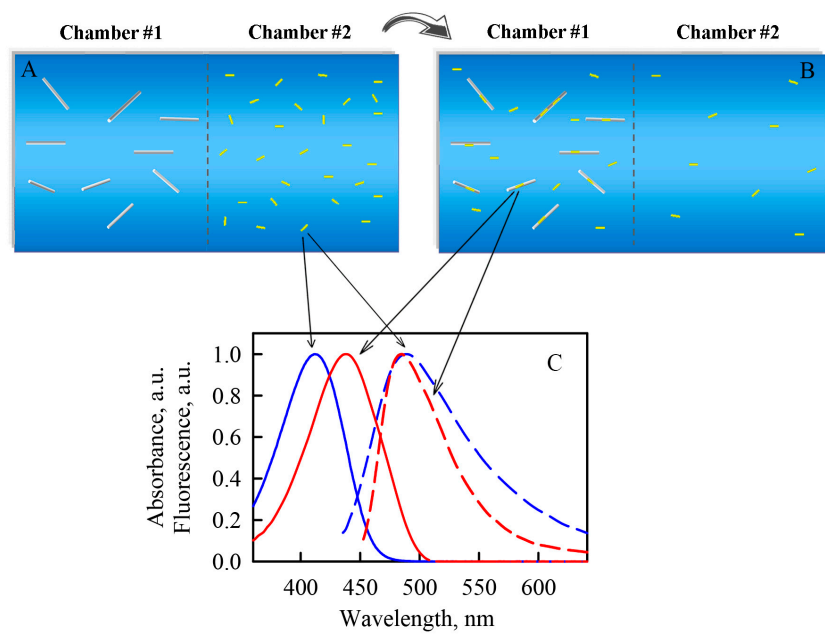
Since the fluorescence quantum yield of free ThT in aqueous solution is very low ( $\sim 0.0001$  [53]), and when the dye binds to fibrils this value may increase in thousand times, it would seem, that to evaluate ThT -  $\alpha$ -synuclein amyloid fibrils binding parameters, one can use the dependence of the fluorescence intensity of ThT in the presence of amyloid fibrils ( $F$ ) on its concentration. However, it should be noted that the solution of ThT with fibrils is an equilibrium system of free ( $C_f$ ) and bound to fibrils ( $C_b$ ) dye. In all studies on the characterization of ThT binding to amyloid fibrils for determination of ThT - fibrils binding parameters the total concentration of ThT ( $C_0$ ) was used instead of the concentration of the free dye ( $C_f$ ), as it should be done. Determination of  $C_f$  and  $C_b$ , at first sight, seems to be a very difficult task. However, to solve this problem, we proposed a simple but very effective approach that was developed a long time ago for the study of receptors - ligands interaction but was lately undeservedly forgotten [54]. The essence of this approach is preparation of investigated solutions by the equilibrium microdialysis technique.

Equilibrium microdialysis implies allocation of two interacting agents, a ligand and receptor, in two chambers (#2 and #1, respectively) divided by a membrane permeable for the ligand and impermeable to the receptor. In our case, amyloid fibrils in the buffer solution were placed in chamber #1 and the ThT solution in the same buffer with an initial concentration  $C_0$ , was placed in chamber #2 (Figure 3A). After equilibration, concentrations of free ThT in chambers #1 and #2 become equal ( $C_f$ ), while the total ThT concentration in chamber #1 is greater than that in chamber #2 by the concentration of the bound dye ( $C_b$ ) (Figure 3B). For determination of  $C_f$  and  $C_b$  values absorption spectra of the sample solution containing free and bound to fibrils ThT, and the reference solution containing only free ThT (in a concentration equal to the concentration of free dye in the sample solution) were recorded. For the solutions containing amyloid fibrils, the contribution of the light scattering was taken into account.

To get a visual representation about the number of ThT -  $\alpha$ -synuclein fibrils binding modes the Scatchard dependence using the calculated  $C_f$ ,  $C_b$ , and  $C_p$  (concentration of the protein on the basis of which the amyloid fibrils were prepared) was plotted (Fig. 4 A). The linearity of this dependence indicates the identity of all binding sites, i.e. the existence of one ThT -  $\alpha$ -synuclein amyloid fibrils binding mode ( $i$ ) (hereinafter referred to as «first» binding mode). Thus, the value of the binding constant ( $K_b$ ) and the number of binding sites ( $n$ ) were determined in assumption that  $i = 1$  using the equation:

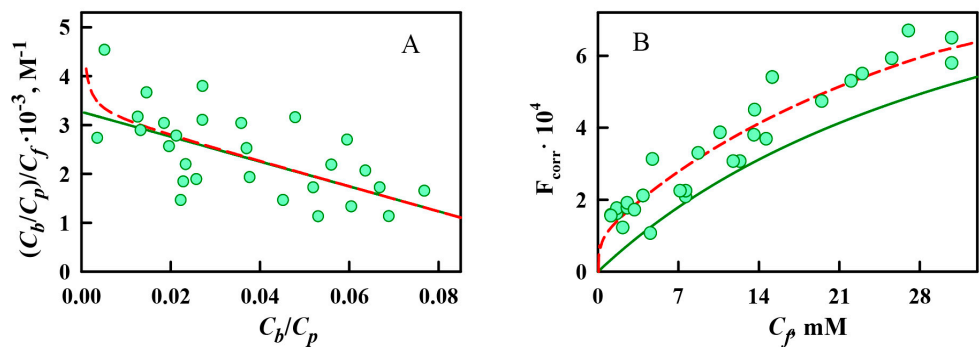
$$C_b = \sum_i \frac{n_i C_p C_f K_{bi}}{1 + C_f K_{bi}}. \quad (1)$$

194



195 **Figure 3.** Determination of photophysical properties of ThT bound to  $\alpha$ -synuclein amyloid fibrils by  
196 the preparation of the sample and reference solutions by equilibrium microdialysis. (A)  $\alpha$ -Synuclein  
197 amyloid fibrils in the buffer solution were placed in chamber #1 and the ThT solution in the same  
198 buffer was placed in chamber #2. (B) After equilibration, free ThT concentrations in chambers #1 and  
199 #2 become equal, while the total ThT concentration in chamber #1 is greater than that in chamber #2  
200 by the concentration of the bound dye. (C) Normalized absorption (solid curves) and fluorescence  
201 (dashed curves) spectra of the free dye in buffer solution (blue curves) and ThT bound to  $\alpha$ -synuclein  
202 amyloid fibrils (blue curves) obtained by the spectroscopic investigation of the solutions after  
203 equilibrium microdialysis.

204 The obtained values of the binding parameters of ThT to  $\alpha$ -synuclein amyloid fibrils as well as  
205 to amyloid fibrils formed from other amyloidogenic proteins are presented in Table 1. It should be  
206 noted that the ThT -  $\alpha$ -synuclein fibrils binding constant has the same order of magnitude as the  
207 binding constant of the dye to the one of modes of other amyloid fibrils, especially formed from  
208 insulin, lysozyme and Abeta-peptide. This fact may indicate the similarity of the mechanism of the  
209  
210



211 **Figure 4.** Determination of ThT –  $\alpha$ -synuclein amyloid fibrils binding parameters. (A) Scatchard plot  
212 and (B) dependence of the corrected on the primary inner filter fluorescence intensity on the  
213 concentration of free ThT are presented. Experimental data (circles) and best-fit curves calculated  
214 with the use of the binding constants ( $K_{bi}$ ) and number of binding sites ( $n_i$ ) values calculated in  
215 assumption of one (green solid curves) and two (red dashed curves) binding modes existence are  
216 given.

dye interaction with these amyloid fibrils. We believe that this type of interaction is due to the incorporation of ThT molecules into the grooves formed by the side chains of amino acids, along the long axis of the fibril perpendicular to  $\beta$ -sheets [55]. However, observed differences in the value of the binding affinity and stoichiometry suggest differences in the structure of this binding sites and consequently in the structure of amyloid fibrils formed from various proteins.

2.3. Photophysical characteristics of ThT bound to alpha-synuclein amyloid fibrils

Spectroscopic investigation of the solutions prepared by equilibrium microdialysis allowed to determine not only the ThT - amyloid fibrils binding parameters, but the characteristics of the bound dye as well. Using the proposed approach absorption spectra of the ThT bound to  $\alpha$ -synuclein amyloid fibrils was determined for the first time (Fig. 3C). As in the case of amyloid fibrils on the basis of other amyloidogenic proteins [41, 43], the absorption spectra of ThT incorporated into  $\alpha$ -synuclein amyloid fibrils are long-wavelength shifted. The red shift of the spectra is associated with a change in ThT microenvironment (an increase in its hydrophobicity).

Using the obtained values of absorbance ( $A_b$ ) and concentration ( $C_b$ ) of ThT bound to  $\alpha$ -synuclein amyloid fibrils, the value of the molar extinction coefficient of bound ThT ( $\epsilon_b$ ) was determined for the first time. The obtained results indicate that ThT binding to  $\alpha$ -synuclein amyloid fibrils along with red-shift of its absorption spectra is accompanied by the decrease in the dye molar extinction coefficient (Table 1). These alterations might be associated with the different conformations of bound to amyloid fibrils and free ThT molecules and their different microenvironment in various conditions.

In the next step, prepared solutions were investigated by fluorescence spectroscopy. Using of the sample and reference solutions obtained by equilibrium microdialysis fluorescence spectra of ThT bound to amyloid fibrils were determined. The position of the fluorescence spectrum of ThT bound to amyloid fibrils coincides with the position of the spectrum of the monomer dye in aqueous solution (Fig. 3C). This fact confirms the monomeric form of the dye binding to amyloid fibrils [56]. The recorded values of fluorescence intensity were corrected on the primary inner filter effect with the use of the specially developed approach [42]. This allowed to determine the fluorescence quantum yield of ThT bound to  $\alpha$ -synuclein amyloid fibrils (see Table 1). It can be noted that its value is in 2 orders of magnitude greater than the fluorescence quantum yield of the free dye in aqueous solution. The increase of the fluorescence quantum yield of ThT bound to amyloid fibrils is caused by the molecular rotor nature of the dye. Rotation of ThT benzothiazole and aminobenzene rings relative to each other in the excited state leads to the dye conformation with the disturbed  $\pi$ -electron conjugated system ( $\varphi \approx 90^\circ$ ) of these fragments and, consequently, to the radiation-less deactivation of the excited state of free ThT molecules in solution [53].

**Table 1.** Characteristics of thioflavin T (ThT) bound to amyloid fibrils and free dye in water solution

Conditions	$\lambda_{abs\_max},$ nm	mode	$\epsilon_{i, max} \times 10^{-4},$ $M^{-1}cm^{-1}$	$K_{bi} \times 10^{-5},$ $M^{-1}$	$n_i$	$q_i$
Alfa-synuclein fibrils (by absorption spectroscopy)	439	1	2.0	0.3	0.13	0.02
Alfa-synuclein fibrils (by absorption and fluorescence spectroscopy)	439	1	2.0	0.3	0.13	0.02
		2	7.0	70	0.0004	0.13
Insulin fibrils [41]	450	1	2.3	0.4	0.14	0.27
		2	7.9	78	0.02	0.72
Lysozyme fibrils [41]	449	1	6.2	0.6	0.25	0.0001
		2	5.3	72	0.11	0.44
$A\beta$ 42 fibrils [41]	440	1	1.4	0.2	0.26	0.03
		2	8.7	70	0.004	0.18
Free in aqueous solution [53]	412	-	3.2	-	-	0.0001

The fluorescent quantum yield increase can be caused by restriction of the ThT fragments rotation relative to each other on the dye incorporation into the "grooves" of amyloid fibrils.

It was also shown that ThT binding to  $\alpha$ -synuclein amyloid fibrils is accompanied by the dye fluorescence lifetime increase about 3 orders of magnitude in comparison of that of free dye (that is about 0.001 ns [57]) (Fig. 5A). In aqueous solutions, the rate of ThT fragments rotation is much higher than the rotation of ThT molecule as a whole, and the fluorescence lifetime is determined by the rate of internal rotation of benzothiazole and aminobenzene rings relative to each other. The restriction of the rotational motions of ThT fragments in the excited state and the decrease of the rate of the radiation-less deactivation of the dye molecules when the dye binds to amyloid fibrils can lead to a significant increase in ThT fluorescent lifetime.

At the same time, it was shown that fluorescence anisotropy of ThT incorporated into  $\alpha$ -synuclein amyloid fibrils remains unchanged (Fig. 5B). This is due to the fact that the dye anisotropy in aqueous medium is close to the upper limiting value (is about 0.38 [57]). Direction of the transition dipole moment of ThT coincides with the axis of the internal rotation of the benzothiazole and aminobenzene rings relative to each other. Therefore, the relative rotation of fragments cannot change the direction of the transition dipole moment of ThT. As relative rotation of the dye fragments (that leads to radiation-less deactivation of the dye molecules) is two orders of magnitude faster than the rotation of the ThT molecule as a whole, the molecule does not have enough time to change its spatial orientation during the lifetime of the excited state. In the bound to fibrils state the characteristic time of both process (rotations) increases, the fluorescence anisotropy of ThT remains the same high.

2.4. The possibility of one more ThT -  $\alpha$ -synuclein amyloid fibrils binding mode existence

Along with the binding mode with the affinity  $\sim 10^4$  M<sup>-1</sup> in amyloid fibrils on the basis of various proteins another binding mode with higher affinity  $\sim 10^6$  M<sup>-1</sup> (hereinafter referred to as «second» binding mode) can be observed (Table 1). In order to understand the nature of the second binding

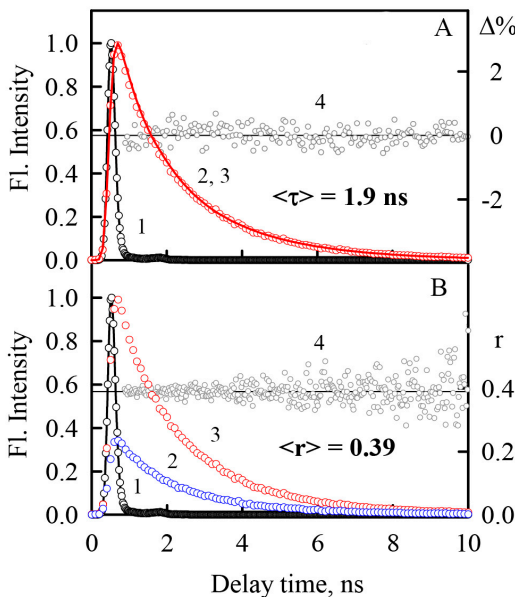


**Figure 5.** Time dependence of fluorescence of ThT bound to  $\alpha$ -synuclein amyloid fibrils. (A) Decay curve of the bound to fibrils dye fluorescence. The instrument response function (1), experimental decay curve of the bound dye fluorescence (2), best fit calculated fluorescence decay curve (3), and deviation between the experimental and calculated decay (4) are shown. The fluorescence decay curve show best fit to a biexponential decay model. (B) Anisotropy of the bound to fibrils dye. The excitation laser impulse profile (1), the decay curves of the vertical (2) and horizontal (3) components of the fluorescence, and the change in fluorescence anisotropy (4) over time are shown.



mode, we analyzed electron micrographs of various amyloid fibrils. It was noted that the fibrils with a single mode of ThT binding represent separate long thin fibers without areas of aggregation (e.g., fibrils on the basis of  $\beta$ -2-microglobulin, shown in Figure 6A), while the fibrils with two ThT binding modes have a propensity to clusterization (e.g., fibrils on the basis of insulin and lysozyme shown in Figure 6B and 6C, respectively). We believe that localization of the dye molecules in these clustered areas of the fibrils (possibly within the above-discussed grooves along the fiber axis) determines the higher binding affinity and more rigid restriction of dye fragments rotation relative to one another and leads to a more significant increase of ThT fluorescence quantum yield in comparison to the case of the first binding mode. Electron microscopy data showed that  $\alpha$ -synuclein amyloid fibrils have clustered areas as well (Fig. 1), however there are less of them and they are much smaller in comparison to that of insulin and lysozyme fibrils in which the binding mode with high affinity was found. Furthermore, confocal microscopy data show different fluorescence intensity of ThT bound to the different areas of  $\alpha$ -synuclein amyloid fibrils (Fig. 7). In this regard, we can assume the possibility of the existence of the second ThT –  $\alpha$ -synuclein amyloid fibrils binding mode, which, however, is difficult to detect by absorption spectroscopy because of a very small number of these binding sites.

We assumed that the second binding mode can be observed by involving the fluorescent spectroscopy results. This assumption is based on the fact that besides absorption, fluorescence intensity depends on the fluorescence quantum yield of the sample. According to our previous results for fibrils formed from other amyloidogenic proteins, the fluorescence quantum yield of ThT bound to a high affinity mode can significantly exceed that of the dye bound to the first mode. This means that, despite the small number of binding sites to the second mode, the molecules interacting with it can have a noticeable contribution to the total fluorescence intensity. To verify this hypothesis it was checked whether the approximation of the experimental fluorescence intensity dependence on the free dye concentration by the calculated curve is satisfactory. The theoretical curve was plotted with the use of the obtained ThT –  $\alpha$ -synuclein fibrils binding parameters in assumption of only one binding mode ( $i = 1$ ) existence:

$$F_{corr} = \sum_i q_{bi} A_{bi} = \sum_i q_{bi} \epsilon_{bi} l C_{bi} = \sum_i q_{bi} \epsilon_{bi} l \frac{n_i C_p C_f K_{bi}}{1 + C_f K_{bi}} \quad (2)$$

Here  $F_{corr}$  is the corrected on the primary inner filter effect fluorescence intensity;  $q_b$  and  $\epsilon_b$  are the quantum yield and molar extinction coefficient of ThT bound to fibrils, respectively;  $l$  is the optical pathlength. Figure 4B shows the mismatch of the experimental and calculated curves that as assumed can be caused by the existence of the second dye binding mode. ThT binding parameters to this mode were determined with the use of equation (2) written in the assumption of existence of two binding modes ( $i = 2$ ) by the multiple nonlinear regression.

When calculating ThT – amyloid fibrils binding parameters it should be taken into account that absorption spectroscopy is a direct method for this aim and provides more accurate results than

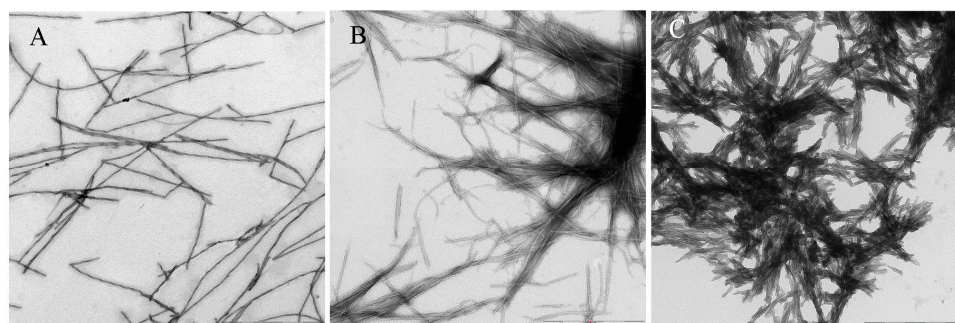


**Figure 6.** Electron micrographs of (A)  $\beta$ -2-microglobulin, (B) insulin and (C) lysozyme amyloid fibrils. Scale bar is 1  $\mu$ m.

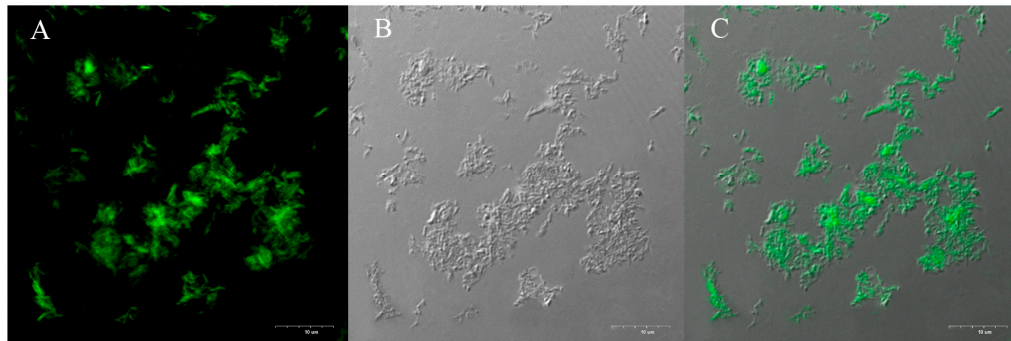


**Figure 7.** Confocal microscopy images of  $\alpha$ -synuclein amyloid fibrils. (A) Fluorescence image of the ThT-stained fibrillar structures, (B) transmitted light image and (C) overlay of these images are shown. Scale bar is 10  $\mu$ m.

fluorescence spectroscopy. Therefore, the calculated by absorption spectroscopy ThT binding parameters to the first mode were fixed during the calculation of binding parameters for the second mode. It should be noted that such calculation is possible due to the preparation of the tested solutions by equilibrium microdialysis, since only this approach allows to calculate the concentration of free dye ( $C_f$ ) in each sample. Furthermore, using the fluorescence intensity correction on the primary inner filter effect is a critical point since an increase in the total concentration of the solution leads to a significant underestimation of the real fluorescence intensity values.

Obtained results (Table 1) show that the number of binding sites to the second mode of  $\alpha$ -synuclein amyloid fibrils is very small as it was expected. On the Figure 4B calculated curves plotted with the use of the obtained binding parameters in assumption of existence of two binding modes ( $i = 2$ ) are shown. Scatchard plots for the cases of one and two binding modes almost coincide. Small differences are observed only in the region of low  $C_0$  values, for which the measurement error is sufficiently high and does not allow correct estimates to be made. At the same time the dependences of the fluorescence intensity on the free dye concentration in these cases differ significantly. This confirms the hypothesis of a greater sensitivity of absorption spectroscopy to the determination of ThT binding parameters to the mode of  $\alpha$ -synuclein amyloid fibrils with the lower affinity and fluorescence spectroscopy for mode of these fibrils with the higher affinity.

With the use of the obtained binding parameters and the results of absorption and fluorescence spectroscopy of solutions prepared by equilibrium microdialysis concentration, molar extinction coefficient and fluorescent quantum yield of the dye bound to the second mode of amyloid fibrils were calculated (Table 1). As expected fluorescence quantum yield of the dye bound to the mode with higher affinity is significantly (almost tenfold) higher than that of ThT bound to the first mode.

### 3. Materials and Methods

#### 3.1. Materials

Thioflavin T (ThT) "UltraPure Grade" from AnaSpec (USA) was used without additional purification. ThT was dissolved in 2 mM Tris-HCl, 150 mM NaCl buffer (pH 7.7). Fluorescent dye ATTO-425 from ATTO-TEC (Germany) and buffer components from Sigma (USA) were used without additional purification.

#### 3.2. $\alpha$ -Synuclein expression and purification

Wild type human  $\alpha$ -synuclein expressed in *E. coli* BL21 cells. The T7-7 plasmid, encoding wild type protein sequence, was used for transformation. This plasmid was a generous gift from Prof. Donna Arndt-Jovin (Max Planck Institute for Biophysical Chemistry, Laboratory of Cellular Dynamics). 100 ml of a pre-culture was inoculated to 900 ml Lysogeny broth (LB) medium with

addition of 1 ml of ampicillin in concentration 100 mg/ml. Incubation was carried out at 37 °C with agitation (400 rpm) until the absorption at wavelength 600 nm reached the value of 0.6-0.8. Expression of the recombinant protein was induced by addition of isopropyl  $\beta$ -D-1-thiogalactopyranoside (IPTG) (0.5 mM) and incubation was continued for an additional 4-6 h. The bacterial cells were harvested by centrifugation (Beckman JA10 rotor, 5000 rpm, 30 min 4 °C) and the pellets were stored at -20 °C. Cell pellets were thawed with 15- 20 ml lysis buffer containing 10 mM Tris-HCl, pH 8.0, 1 mM EDTA and 1 mM protease inhibitor PMSF. The cells were lysed by sonication with Labsonic M apparatus for 30 minutes. The mixture was centrifuged 30 min at 5000 rpm recovering the supernatant. Proteins other than  $\alpha$ -synuclein were precipitated by boiling at 100 °C for 20 min followed by centrifugation at 12000 rpm for 30 min at 4 °C. The pellets containing  $\alpha$ -synuclein were stored at -20 °C. Purification of  $\alpha$ -synuclein was carried out with Mono-Q 10/10 column (Amersham Biosciences).

### 3.3. Investigation of kinetics of amyloid fibrils formation

Solutions of  $\alpha$ -synuclein at pH 3.7 in 0.2 M acetate buffer were stirred at 37 °C in glass vials with micro-stir bars. Protein concentration was 1 mg/ml. Fibril formation was monitored with thioflavin T absorption and fluorescence. The presence of fibrils was confirmed by electron microscopy. Changes in the protein secondary structure were monitored by CD-spectroscopy. The fibrillogenesis was repeated several times to verify the identity of the formed aggregates.

### 3.4. Electron microscopy

To obtain electron micrographs, the method of negative staining with a 1% aqueous solution of uranyl acetate was used. Amyloid fibrils were placed on copper grids coated with a collodion film-substrate. Electron micrographs of amyloid fibrils were obtained using transmission electron microscope Libra 120 (Carl Zeiss, Germany).

### 3.5. Confocal microscopy

For obtaining the fluorescence images of the ThT - stained fibrillar structures the confocal laser scanning microscope Olympus FV 3000 (Olympus, Japan) was used. An objective lens with a 60x magnification and an aperture NA 1.42 was used. For fluorescent probe excitation, the fixed laser line was used (405 nm). Registration of fluorescent light was carried out in the range of 420 – 520 nm. To assess the presence of fibrils in the investigated sample region and the areas of the dye accumulation the transmitted light images was also obtained.

### 3.6. Equilibrium microdialysis

Equilibrium microdialysis was performed with a Harvard Apparatus/Amika (USA) device, which consists of two chambers (500  $\mu$ L each), separated by a membrane (MWCO 10,000) impermeable to particles larger than 10,000 Da. The concentration of amyloid fibrils in each experiment was 0.4 mg/ml.

### 3.6. Absorption spectroscopy

The absorption spectra were recorded using spectrophotometer U-3900H (Hitachi, Japan). The concentration of ThT and  $\alpha$ -synuclein in solutions was determined using a molar extinction coefficients of  $\epsilon_{412} = 31600 \text{ M}^{-1}\text{cm}^{-1}$  (on the basis of our results) and  $\epsilon_{280} = 5120 \text{ M}^{-1}\text{cm}^{-1}$  [58], respectively. Contribution of light scattering to the measured absorption spectra was determined from the relationship:  $A_{\text{scat}} = a\lambda^{-m}$  [59]. Coefficients  $a$  and  $m$  were determined from the linear part of the dependence of  $A$  on  $\lambda$ , where there is no active dye absorption plotted in logarithmical coordinates  $\lg(A_{\text{scat}}) = f(\lg(\lambda))$ .

### 3.7. Fluorescence spectroscopy

Fluorescence measurements were performed with a Cary Eclipse spectrofluorimeter (Varian, Australia). PBS solution of fluorescent dye ATTO-425, whose fluorescence and absorption spectra are similar to that of ThT, was taken as a reference for determining the corrected and normalized values of fluorescence intensity of ThT bound to amyloid fibrils. The fluorescence quantum yield of ATTO-425 is 0.9 (ATTO-TEC Catalogue 2009/2010 p.14). Fluorescence spectra of ThT and ATTO-425 were excited at 435 nm. The spectral slits width was 5 nm in all experiments. Change of spectral slits width did not influence on the experimental results. Registered values of fluorescence intensity were corrected on the primary inner filter effect as described earlier [42].

### 3.8. Time-resolved Fluorescence Measurements

The fluorescence decay curves in the subnanosecond and nanosecond ranges were recorded by a spectrometer FluoTime 300 (Pico Quant, Germany) with the Laser Diode Head LDH-C-440 ( $\lambda_{ex} = 440$  nm). The measured emission decays were fit to a multiexponential function using the standard convolute-and-compare nonlinear least-squares procedure [60]. In this method, the convolution of the model exponential function with the instrument response function (IRF) was compared to the experimental data until a satisfactory fit was obtained. The IRF was measured using cross correlation of the excitation and fundamental gate pulse. The fitting routine was based on the nonlinear least-squares method. Minimization was performed according to Marquardt [61].

Fluorescence anisotropy was determined as:  $r = (F_V^V - GF_H^V) / (F_V^V + 2GF_H^V)$ , where  $F_V^V$  and  $F_H^V$  are vertical and horizontal components of fluorescence intensity excited by vertical polarized light, and  $G = F_V^H / F_H^H$  is coefficient which determines the different sensitivity of the registering system for vertical and horizontal components of fluorescence intensity.

### 3.9. CD spectroscopy

CD spectra in the far UV-region were measured using a J-810 spectropolarimeter (Jasco, Japan). Spectra were recorded in a 0.1-cm cell from 250 to 190 nm. For all spectra, an average of three scans was obtained. CD spectrum of the appropriate buffer was recorded and subtracted from the protein spectra.

## 4. Conclusions

In this work, a novel approach based on the preparation of the tested solutions by equilibrium microdialysis for the study of the ThT-  $\alpha$ -synuclein amyloid fibrils interaction was applied. Using this method allowed to identify two types (modes) of the dye binding to  $\alpha$ -synuclein fibrils with significantly different binding parameters. A greater sensitivity of absorption spectroscopy to the determination of ThT binding parameters to the mode with the lower affinity and fluorescence spectroscopy for the mode with the higher affinity was shown. A very small number of the dye binding sites for the mode with the higher affinity (1 ThT / 2500  $\alpha$ -synuclein molecules) compared with the mode with lower affinity (1 ThT / 8  $\alpha$ -synuclein molecules) was shown. It should be noted that the information about ThT -  $\alpha$ -synuclein amyloid fibrils stoichiometry can be used for estimating the correct dye/fibrils ratio in experiments on detection of this protein fibrillation.

Using of the proposed approach for tested solutions preparation allowed as well to indicate significant differences of the photophysical characteristics of the dye bound to the sites of different binding modes. Analysis of the obtained results led to the suggestion that the existence of one of these modes (with lower affinity) is caused by the incorporation of the dye into the grooves formed by the side chains of amino acids, along the long axis of the fibril perpendicular to  $\beta$ -sheets. Comparison of ThT binding parameters to amyloid fibrils formed from different proteins and analysis of their images obtained by electron microscopy allowed to assume that the existence of



another mode can be caused by the localization of the dye molecules in the clustered areas of the fibrils (possibly within the above-discussed grooves along the fiber axis). The present hypothesis suggests low accessibility of this mode binding sites and rigid restriction of rotation of the dye fragments relative to each other. This is in a good agreement with the data of a high ThT-fibrils binding affinity and low stoichiometry to this mode, as well as high fluorescence quantum yield and lifetime of the bound dye. This assumption is also confirmed by the results of confocal microscopy of  $\alpha$ -synuclein amyloid fibrils in the presence of ThT.

The results of this work, which made it possible to show for the first time the presence of two modes of ThT binding to  $\alpha$ -synuclein amyloid fibrils and characterize each of them, are currently relevant, since fluorescent probes including ThT, its analogues and derivatives are considered as diagnostic and therapeutic agents. Special attention in experiments *in vitro* should be given the exact characterization of the second ThT - amyloid fibrils binding type (mode), because in the brain of patients with Parkinson's disease  $\alpha$ -synuclein amyloid fibrils predominantly do not represent individual fibers but are a part of the pathological plaques (Lewy bodies). The formation of clusters can be a factor determining the amyloid fibrils cytotoxicity or mechanism of their effect on the cells. Thereby in the case of such pathologies the interaction of fluorescent probes with clusters and aggregates of amyloid fibrils can dominate over the interaction with individual fine filaments. In this regard, the results of the work may be in demand when developing approaches for determination of the number of binding types of fluorescent probes to amyloid fibrils, characterization of these modes and estimation which of them is predominant in pathologies.

**Funding:** This work was supported by the "Molecular and Cell Biology" Program of the Russian Academy of Sciences, Russian Foundation of Basic Research (grant number 16-04-01614, 18-34-00975) and the RF President Fellowship (number SP-841.2018.4).

**Author Contributions:** Conceptualization and Supervision K.T., I.K.; Methodology, K.T., I.K., A.S.; Investigation and Visualization A.S., N.R., M.S., O.P., I.A.; Writing – Original Draft Preparation, Review & Editing, A.S., N.R., M.S., O.P., I.A., I.K., K.T.

**Conflicts of Interest:** The authors declare no conflict of interest.

## References

1. Ueda, K.; Fukushima, H.; Masliah, E.; Xia, Y.; Iwai, A.; Yoshimoto, M.; Otero, D. A.; Kondo, J.; Ihara, Y.; Saitoh, T., Molecular cloning of cDNA encoding an unrecognized component of amyloid in Alzheimer disease. *Proceedings of the National Academy of Sciences of the United States of America* **1993**, 90, (23), 11282-6.
2. Jakes, R.; Spillantini, M. G.; Goedert, M., Identification of two distinct synucleins from human brain. *FEBS letters* **1994**, 345, (1), 27-32.
3. Lavedan, C., The synuclein family. *Genome research* **1998**, 8, (9), 871-80.
4. Duda, J. E.; Shah, U.; Arnold, S. E.; Lee, V. M.; Trojanowski, J. Q., The expression of alpha-, beta-, and gamma-synucleins in olfactory mucosa from patients with and without neurodegenerative diseases. *Experimental neurology* **1999**, 160, (2), 515-22.
5. Nakai, M.; Fujita, M.; Waragai, M.; Sugama, S.; Wei, J.; Akatsu, H.; Ohtaka-Maruyama, C.; Okado, H.; Hashimoto, M., Expression of alpha-synuclein, a presynaptic protein implicated in Parkinson's disease, in erythropoietic lineage. *Biochemical and biophysical research communications* **2007**, 358, (1), 104-10.
6. Barbour, R.; Kling, K.; Anderson, J. P.; Banducci, K.; Cole, T.; Diep, L.; Fox, M.; Goldstein, J. M.; Soriano, F.; Seubert, P.; Chilcote, T. J., Red blood cells are the major source of alpha-synuclein in blood. *Neuro-degenerative diseases* **2008**, 5, (2), 55-9.
7. Li, Q. X.; Campbell, B. C.; McLean, C. A.; Thyagarajan, D.; Gai, W. P.; Kapsa, R. M.; Beyreuther, K.; Masters, C. L.; Culvenor, J. G., Platelet alpha- and gamma-synucleins in Parkinson's disease and normal control subjects. *Journal of Alzheimer's disease : JAD* **2002**, 4, (4), 309-15.

8. Michell, A. W.; Luheshi, L. M.; Barker, R. A., Skin and platelet alpha-synuclein as peripheral biomarkers of Parkinson's disease. *Neuroscience letters* **2005**, 381, (3), 294-8.
9. Noori-Dalooi, M. R.; Kheirollahi, M.; Mahbod, P.; Mohammadi, F.; Astaneh, A. N.; Zarindast, M. R.; Azimi, C.; Mohammadi, M. R., Alpha- and beta-synucleins mRNA expression in lymphocytes of schizophrenia patients. *Genetic testing and molecular biomarkers* **2010**, 14, (5), 725-9.
10. Alim, M. A.; Hossain, M. S.; Arima, K.; Takeda, K.; Izumiyama, Y.; Nakamura, M.; Kaji, H.; Shinoda, T.; Hisanaga, S.; Ueda, K., Tubulin seeds alpha-synuclein fibril formation. *The Journal of biological chemistry* **2002**, 277, (3), 2112-7.
11. Zhu, M.; Qin, Z. J.; Hu, D.; Munishkina, L. A.; Fink, A. L., Alpha-synuclein can function as an antioxidant preventing oxidation of unsaturated lipid in vesicles. *Biochemistry* **2006**, 45, (26), 8135-42.
12. George, J. M.; Jin, H.; Woods, W. S.; Clayton, D. F., Characterization of a novel protein regulated during the critical period for song learning in the zebra finch. *Neuron* **1995**, 15, (2), 361-72.
13. Bonini, N. M.; Giasson, B. I., Snaring the function of alpha-synuclein. *Cell* **2005**, 123, (3), 359-61.
14. Cooper, A. J.; Jeitner, T. M.; Blass, J. P., The role of transglutaminases in neurodegenerative diseases: overview. *Neurochemistry international* **2002**, 40, (1), 1-5.
15. Breydo, L.; Wu, J. W.; Uversky, V. N., Alpha-synuclein misfolding and Parkinson's disease. *Biochimica et biophysica acta* **2012**, 1822, (2), 261-85.
16. Ekman, D.; Light, S.; Bjorklund, A. K.; Elofsson, A., What properties characterize the hub proteins of the protein-protein interaction network of *Saccharomyces cerevisiae*? *Genome biology* **2006**, 7, (6), R45.
17. Weinreb, P. H.; Zhen, W.; Poon, A. W.; Conway, K. A.; Lansbury, P. T., Jr., NACP, a protein implicated in Alzheimer's disease and learning, is natively unfolded. *Biochemistry* **1996**, 35, (43), 13709-15.
18. Cote, Y.; Delarue, P.; Scheraga, H. A.; Senet, P.; Maisuradze, G. G., From a Highly Disordered to a Metastable State: Uncovering Insights of alpha-Synuclein. *ACS chemical neuroscience* **2018**.
19. Fakhree, M. A. A.; Nolten, I. S.; Blum, C.; Claessens, M., Different Conformational Subensembles of the Intrinsically Disordered Protein alpha-Synuclein in Cells. *The journal of physical chemistry letters* **2018**, 9, (6), 1249-1253.
20. Ferreon, A. C.; Gambin, Y.; Lemke, E. A.; Deniz, A. A., Interplay of alpha-synuclein binding and conformational switching probed by single-molecule fluorescence. *Proceedings of the National Academy of Sciences of the United States of America* **2009**, 106, (14), 5645-50.
21. Veldhuis, G.; Segers-Nolten, I.; Ferlemann, E.; Subramaniam, V., Single-molecule FRET reveals structural heterogeneity of SDS-bound alpha-synuclein. *Chembiochem : a European journal of chemical biology* **2009**, 10, (3), 436-9.
22. Nuscher, B.; Kamp, F.; Mehnert, T.; Odoy, S.; Haass, C.; Kahle, P. J.; Beyer, K., Alpha-synuclein has a high affinity for packing defects in a bilayer membrane: a thermodynamics study. *The Journal of biological chemistry* **2004**, 279, (21), 21966-75.
23. Pfefferkorn, C. M.; Jiang, Z.; Lee, J. C., Biophysics of alpha-synuclein membrane interactions. *Biochimica et biophysica acta* **2012**, 1818, (2), 162-71.
24. Wang, W.; Perovic, I.; Chittuluru, J.; Kaganovich, A.; Nguyen, L. T.; Liao, J.; Auclair, J. R.; Johnson, D.; Landeru, A.; Simorellis, A. K.; Ju, S.; Cookson, M. R.; Asturias, F. J.; Agar, J. N.; Webb, B. N.; Kang, C.; Ringe, D.; Petsko, G. A.; Pochapsky, T. C.; Hoang, Q. Q., A soluble alpha-synuclein construct forms a dynamic tetramer. *Proceedings of the National Academy of Sciences of the United States of America* **2011**, 108, (43), 17797-802.
25. Lassen, L. B.; Reimer, L.; Ferreira, N.; Betzer, C.; Jensen, P. H., Protein Partners of alpha-Synuclein in Health and Disease. *Brain pathology* **2016**, 26, (3), 389-97.

- 554 26. Paleologou, K. E.; El-Agnaf, O. M., alpha-Synuclein aggregation and modulating factors.  
555 *Sub-cellular biochemistry* **2012**, 65, 109-64.
- 556 27. Wood, S. J.; Wypych, J.; Steavenson, S.; Louis, J. C.; Citron, M.; Biere, A. L., alpha-synuclein  
557 fibrillogenesis is nucleation-dependent. Implications for the pathogenesis of Parkinson's  
558 disease. *The Journal of biological chemistry* **1999**, 274, (28), 19509-12.
- 559 28. Iljina, M.; Garcia, G. A.; Horrocks, M. H.; Tosatto, L.; Choi, M. L.; Ganzinger, K. A.;  
560 Abramov, A. Y.; Gandhi, S.; Wood, N. W.; Cremades, N.; Dobson, C. M.; Knowles, T. P.;  
561 Klenerman, D., Kinetic model of the aggregation of alpha-synuclein provides insights into  
562 prion-like spreading. *Proceedings of the National Academy of Sciences of the United States of*  
563 *America* **2016**, 113, (9), E1206-15.
- 564 29. Dearborn, A. D.; Wall, J. S.; Cheng, N.; Heymann, J. B.; Kajava, A. V.; Varkey, J.; Langen, R.;  
565 Steven, A. C., alpha-Synuclein Amyloid Fibrils with Two Entwined, Asymmetrically  
566 Associated Protofibrils. *The Journal of biological chemistry* **2016**, 291, (5), 2310-8.
- 567 30. Zhang, H.; Griggs, A.; Rochet, J. C.; Stanciu, L. A., In vitro study of alpha-synuclein  
568 protofibrils by cryo-EM suggests a Cu(2+)-dependent aggregation pathway. *Biophysical*  
569 *journal* **2013**, 104, (12), 2706-13.
- 570 31. Naiki, H.; Higuchi, K.; Hosokawa, M.; Takeda, T., Fluorometric determination of amyloid  
571 fibrils in vitro using the fluorescent dye, thioflavin T1. *Anal. Biochem.* **1989**, 177, (2), 244-9.
- 572 32. LeVine, H., 3rd, Thioflavine T interaction with synthetic Alzheimer's disease beta-amyloid  
573 peptides: detection of amyloid aggregation in solution. *Protein Sci.* **1993**, 2, (3), 404-10.
- 574 33. LeVine, H., 3rd, Quantification of beta-sheet amyloid fibril structures with thioflavin T.  
575 *Methods Enzymol.* **1999**, 309, 274-84.
- 576 34. Wu, C.; Biancalana, M.; Koide, S.; Shea, J. E., Binding Modes of Thioflavin-T to the  
577 Single-Layer beta-Sheet of the Peptide Self-Assembly Mimics. *J. Mol. Biol.* **2009**.
- 578 35. Biancalana, M.; Makabe, K.; Koide, A.; Koide, S., Molecular mechanism of thioflavin-T  
579 binding to the surface of beta-rich peptide self-assemblies. *J. Mol. Biol.* **2009**, 385, (4),  
580 1052-63.
- 581 36. Biancalana, M.; Koide, S., Molecular mechanism of Thioflavin-T binding to amyloid fibrils.  
582 *Biochimica et biophysica acta* **2010**, 1804, (7), 1405-12.
- 583 37. Morimoto, K.; Kawabata, K.; Kunii, S.; Hamano, K.; Saito, T.; Tonomura, B.,  
584 Characterization of type I collagen fibril formation using thioflavin T fluorescent dye. *J*  
585 *Biochem* **2009**, 145, (5), 677-84.
- 586 38. Ye, L.; Velasco, A.; Fraser, G.; Beach, T. G.; Sue, L.; Osredkar, T.; Libri, V.; Spillantini, M. G.;  
587 Goedert, M.; Lockhart, A., In vitro high affinity alpha-synuclein binding sites for the  
588 amyloid imaging agent PIB are not matched by binding to Lewy bodies in postmortem  
589 human brain. *Journal of neurochemistry* **2008**, 105, (4), 1428-1437.
- 590 39. Groenning, M.; Norrman, M.; Flink, J. M.; van de Weert, M.; Bukrinsky, J. T.; Schluckebier,  
591 G.; Frokjaer, S., Binding mode of Thioflavin T in insulin amyloid fibrils. *J. Struct. Biol.* **2007**,  
592 159, (3), 483-97.
- 593 40. Groenning, M., Binding mode of Thioflavin T and other molecular probes in the context of  
594 amyloid fibrils-current status. *J. Chem. Biol.* **2009**, DOI 10.1007/s12154-009-0027-5.
- 595 41. Kuznetsova, I. M.; Sulatskaya, A. I.; Uversky, V. N.; Turoverov, K. K., A new trend in the  
596 experimental methodology for the analysis of the thioflavin T binding to amyloid fibrils.  
597 *Molecular neurobiology* **2012**, 45, (3), 488-98.
- 598 42. Fonin, A. V.; Sulatskaya, A. I.; Kuznetsova, I. M.; Turoverov, K. K., Fluorescence of dyes in  
599 solutions with high absorbance. Inner filter effect correction. *PloS one* **2014**, 9, (7), e103878.
- 600 43. Sulatskaya, A. I.; Kuznetsova, I. M.; Belousov, M. V.; Bondarev, S. A.; Zhouravleva, G. A.;  
601 Turoverov, K. K., Stoichiometry and Affinity of Thioflavin T Binding to Sup35p Amyloid  
602 Fibrils. *PloS one* **2016**, 11, (5), e0156314.
- 603 44. Sulatskaya, A. I.; Povarova, O. I.; Kuznetsova, I. M.; Uversky, V. N.; Turoverov, K. K.,  
604 Binding stoichiometry and affinity of fluorescent dyes to proteins in different structural  
605 states. *Methods in molecular biology* **2012**, 895, 441-60.

- 606 45. Uversky, V. N.; Li, J.; Fink, A. L., Evidence for a partially folded intermediate in  
607 alpha-synuclein fibril formation. *The Journal of biological chemistry* **2001**, 276, (14), 10737-44.
- 608 46. Kjaergaard, M.; Norholm, A. B.; Hendus-Altenburger, R.; Pedersen, S. F.; Poulsen, F. M.;  
609 Kragelund, B. B., Temperature-dependent structural changes in intrinsically disordered  
610 proteins: formation of alpha-helices or loss of polyproline II? *Protein science : a publication of*  
611 *the Protein Society* **2010**, 19, (8), 1555-64.
- 612 47. Ban, T.; Hamada, D.; Hasegawa, K.; Naiki, H.; Goto, Y., Direct observation of amyloid fibril  
613 growth monitored by thioflavin T fluorescence. *The Journal of biological chemistry* **2003**, 278,  
614 (19), 16462-5.
- 615 48. Selivanova, O. M.; Glyakina, A. V.; Gorbunova, E. Y.; Mustaeva, L. G.; Suvorina, M. Y.;  
616 Grigorashvili, E. I.; Nikulin, A. D.; Dovidchenko, N. V.; Rekstina, V. V.; Kalebina, T. S.;  
617 Surin, A. K.; Galzitskaya, O. V., Structural model of amyloid fibrils for amyloidogenic  
618 peptide from Bgl2p-glucantransferase of *S. cerevisiae* cell wall and its modifying analog.  
619 New morphology of amyloid fibrils. *Biochimica et biophysica acta* **2016**, 1864, (11), 1489-99.
- 620 49. Zahn, R., Prion propagation and molecular chaperones. *Q Rev Biophys* **1999**, 32, (4), 309-70.
- 621 50. Dobson, C. M., Protein folding and misfolding. *Nature* **2003**, 426, (6968), 884-90.
- 622 51. Dobson, C. M., Experimental investigation of protein folding and misfolding. *Methods* **2004**,  
623 34, (1), 4-14.
- 624 52. Sunde, M.; Serpell, L. C.; Bartlam, M.; Fraser, P. E.; Pepys, M. B.; Blake, C. C., Common core  
625 structure of amyloid fibrils by synchrotron X-ray diffraction. *Journal of molecular biology*  
626 **1997**, 273, (3), 729-39.
- 627 53. Sulatskaya, A. I.; Maskevich, A. A.; Kuznetsova, I. M.; Uversky, V. N.; Turoverov, K. K.,  
628 Fluorescence quantum yield of thioflavin T in rigid isotropic solution and incorporated into  
629 the amyloid fibrils. *PloS one* **2010**, 5, (10), e15385.
- 630 54. Oravcova, J.; Bohs, B.; Lindner, W., Drug-protein binding sites. New trends in analytical  
631 and experimental methodology. *J Chromatogr B Biomed Appl* **1996**, 677, (1), 1-28.
- 632 55. Krebs, M. R.; Bromley, E. H.; Donald, A. M., The binding of thioflavin-T to amyloid fibrils:  
633 localisation and implications. *J. Struct. Biol.* **2005**, 149, (1), 30-7.
- 634 56. Sulatskaya, A. I.; Lavysheva, A. V.; Maskevich, A. A.; Kuznetsova, I. M.; Turoverov, K. K.,  
635 Thioflavin T fluoresces as excimer in highly concentrated aqueous solutions and as  
636 monomer being incorporated in amyloid fibrils. *Scientific reports* **2017**, 7, (1), 2146.
- 637 57. Kuznetsova, I. M.; Sulatskaya, A. I.; Maskevich, A. A.; Uversky, V. N.; Turoverov, K. K.,  
638 High Fluorescence Anisotropy of Thioflavin T in Aqueous Solution Resulting from Its  
639 Molecular Rotor Nature. *Analytical chemistry* **2016**, 88, (1), 718-24.
- 640 58. Grabenauer, M.; Bernstein, S. L.; Lee, J. C.; Wytenbach, T.; Dupuis, N. F.; Gray, H. B.;  
641 Winkler, J. R.; Bowers, M. T., Spermine binding to Parkinson's protein alpha-synuclein and  
642 its disease-related A30P and A53T mutants. *The journal of physical chemistry. B* **2008**, 112,  
643 (35), 11147-54.
- 644 59. Vladimirov, Y. A.; Litvin, F. F., Photobiology and spectroscopic methods. *Handbook of*  
645 *general biophysics* **1964**, 8.
- 646 60. O'Connor, D. V. P., D., Time-correlated Single Photon Counting. *New-York, Academic Press*  
647 **1984**, 37-54.
- 648 61. Marquardt, D. W., An algorithm for least-squares estimation of non linear parameters. *J.*  
649 *Soc. Ind. Appl. Math.* **1963**, 11, 431-441.